Scientific Research Publishing

Open Journal of Physical Chemistry, 2024, 14, 1-20
https://www.scirp.org/journal/ojpc
ISSN Online: 2162-1977
ISSN Print: 2162-1969

Efficient Sequestration of Congo Red Dye from Aqueous Solutions Using Pamam Dendrimer-Silica Composite

Augustus Ebelegi[1], Nimibofa Ayawei[2], Donbebe Wankasi[1]

[1]Department of Chemical Sciences, Niger Delta University, Wilberforce Island, Nigeria
[2]Department of Chemistry, Bayelsa Medical University, Yenagoa, Nigeria
Email: ayawei4acad@gmail.com

How to cite this paper: Ebelegi, A., Ayawei, N. and Wankasi, D. (2024) Efficient Sequestration of Congo Red Dye from Aqueous Solutions Using Pamam Dendrimer-Silica Composite. *Open Journal of Physical Chemistry*, **14**, 1-20.
https://doi.org/10.4236/ojpc.2024.141001

Received: February 1, 2024
Accepted: February 26, 2024
Published: February 29, 2024

Abstract

This study investigates the removal of Congo Red dye from aqueous solution using functionalized generation 3.0 and 5.0 polyamidoamine dendrimer-silica gel composite (G-3PS, G-5PS). Fourier Transform-Infra Red spectroscopy, Brunauer Emmett and Teller, Thermo Gravimetric Analysis, pH at point of zero charge, and scanning electron microscopy measurements have been applied to characterize the synthetic nanohybrid composite, these techniques revealed the successful functionalization of both dendrimer molecules and subsequent immobilization onto silica gel. The implications of varying adsorption parameters such as contact time, initial concentration of adsorbate, temperature and pH on both composites were studied. Experimental data obtained from batch adsorption processes were fitted into two equilibrium isotherms (Langmuir and Freundlich) and 3 kinetic models (Pseudo-First-Order, Pseudo-Second-Order, Intra Particle Diffusion). Adsorption mechanism was mainly governed by film diffusion due to electrostatic interactions between the functionalized dendrimer surface and Congo Red molecules. Thermodynamic parameters illustrate that the adsorption is endothermic and spontaneous. Findings suggest the Nanocomposites (G-3PS and G-5PS) are good adsorbents for the removal of Congo Red dye from aqueous solutions.

Keywords

Dendrimer, Langmuir, Freundlich, Adsorption Mechanism, Intra Particle Diffusion, Nano-Composites

1. Introduction

Studies have shown that there are more than 100,000 commercially available

dyes in circulation and more than 7×10^5 tonnes per year are produced annually [1] [2]. Industrial effluents containing dyes are very tricky to treat because they are recalcitrant organic molecules that are resistant to aerobic digestion but stable to light. Synthetic dyes cannot be efficiently cleaned from industrial effluents by traditional methods because of their complex structure and synthetic origin [3]. Congo Red (CR) (sodium salt of benzidinediazobis-1-naphthylamine-4-sulfonic acid) is a benzidine-based azo dye. It was the first synthetic dye produced that was capable of dyeing cotton easily; Congo Red is very sensitive to acids, its colour changes from red to blue in the presence of inorganic acids [4]. Congo Red is synthesized by coupling tetrazotized Benzidine with two molecules of Naphtionic acid [5]. It mainly occurs in the effluents discharged from textile, paper, printing, and leather industries. About 15% of Congo Red ends up in wastewaters and thus there are many processes to remove Congo Red molecules from colored effluents and the treatment methods can be divided into three categories namely; physical methods such as adsorption, chemical methods such as ozonation, electrochemical process and biodegradation [6]. Congo Red dye was chosen for this study because of its complex chemical structure, high solubility in aqueous solution and persistence when discharged into the natural environment. Congo Red is usually metabolized to benzidine, and is known to have toxic, mutagenic, carcinogenic and teratogenic properties [7].

Although secondary pollution challenges have been identified as common disadvantages of most conventional dye sequestration techniques, the use of hybrid adsorbent composites having multiple functions (enzyme degradation, good adsorption properties look promising) [1] [2] [8]. The practice of utilizing material composites for enhanced adsorption of dyes from aqueous solution is well-reported in literature [8] [9].

In this study Generation-3 and Generation-5 Polyamidoamine dendrimers were functionalized with Succinic anhydride and subsequently immobilized on silica gel using a linker, (3-aminopropyl) triethoxysilane (APTES) to produce two composites (G-3PS and G-5PS) that were further characterized to reveal their physicochemical properties. Scientific reports have it that specifically designed properties can be integrated into silica backbone [10] [11] as such there is a growing interest in the chemistry of amalgamating active moieties onto silica in order to achieve desired structural and functional characteristics. The focal point of this study is to experiment uptake of Congo Red dye by the prepared adsorbents in aqueous solutions under optimized reaction conditions of contact time, pH, initial concentration and temperature.

2. Materials and Method

2.1. Synthesis of Adsorbents (G-3PS and G-5PS)

The listed analytical grade chemicals were used throughout the study; Generation-3 and Generation-5 Polyamidoamine (PAMAM) dendrimers with ethylenediamine core, succinic anhydride, (3-aminopropyl) triethoxysilane (APTES), silica gel (particle size-240-425 mesh, pore size-15 nm), pH-7, pore volume (1.15

cm^3/g) were obtained from Sigma Aldrich. Congo Red powder and *N*-(3-dimethylaminopropyl-*N'*-ethylcarbodiimide hydrochloride and were obtained from Merck and Thermo fisher scientific respectively.

The linker, 3-aminopropyltriethoxysilane (APTES) was implanted on the silica gel using similar methods previously illustrated by Acres *et al.* [12]. Silica gel (30 g) was at first activated by oven drying at 130˚C for 2 h. Then twenty gram of the activated silica gel was refluxed at 115˚C for 6 h within a binary mixture made up of 10% APTES in 100 mL anhydrous toluene. The product obtained after reflux is the amino-propyl-functionalized silica. This product (amino-propyl-functionalized silica) was separated from the solution by centrifugation at 4000 rpm for 10 min. The amino functionalized silica was washed with water and ethanol (alternatively) to remove any remaining preparation reagents. The finishing wash was with ethanol followed by oven drying at 105˚C for 1 h. The amino-propyl-functionalized silica was labeled SG-APTES, and stored in a clean bottle for later use.

PAMAM dendrimers with Succinic acid terminals were prepared by adopting a method previously used by Shi *et al.* [13]. This was done in order to synthesize PAMAM functionalized silica (G-3PS and G-5PS) by means of a condensation reaction between the Succinic terminal and the amine terminal of the SG-APTES. The Succinic acid terminated PAMAM dendrimers were prepared by dissolving approximately 3.7 mL of G-3 or G-5 PAMAM dendrimers and 3.1 g Succinic anhydride in separate 50 mL volumes of dimethyl sulfoxide (DMSO). Both solutions were then refluxed at 80˚C for 12 h and later dialyzed with deionized water over 3 d (the deionized water was replaced every 6 h). The Succinic acid terminated G-3 or G-5 PAMAM dendrimers were withdrawn from the dialysis system and stored for further use.

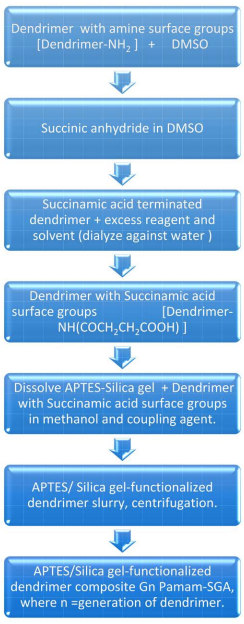

Figure 1. Generic schematics for the synthesis of G-3PS and G-5PS.

A method previously employed by Jiang *et al.* [14] was utilized in the experimental procedure used to affix the SG-APTES to the succinic acid terminated generations-3 and 5 PAMAM dendrimers. The SLC-APTES (20 g) and succinic acid terminated PAMAM dendrimers (20 mL) were mixed in a 250 mL round bottom flask containing 75 mL methanol. The coupling agent *N*-(3-dimethylaminopropyl)-*N'*-ethylcarbodiimide hydrochloride (EDC) (≈5 mg) was added to the flask and the entire mixture was refluxed at 90˚C for 12 h. The product was separated from the solution by centrifugation at 4000 rpm for 10 min. It was washed thrice with ethanol and dried at 110˚C for 1 h. The final products are the G-3 PAMAM functionalized silica (G-3PS) and G-5 PAMAM functionalized silica (G-5PS) (see **Figure 1**).

2.2. Characterization of the Adsorbents

The G-3PS, G-5PS and some pristine silica gel were characterized using fourier transform infrared (FTIR) spectrometer (Spectrum Two, Perkin Elmer Instruments, USA). Micromeritics TRISTAR II 3020 analyzer (Micromeritics Instrument Corporation, USA) was used to detect surface area and porosity, Thermo-gravimetric analyzer (Perkin-Elmer TGA 4000, Perkin Elmer Instruments, USA) was used for the Thermo-gravimetric analysis (TGA) in order to determine the stability of adsorbents, and the scanning electron microscope (SEM) (Zeiss Auriga Field Emission) was used to determine the surface morphology.

2.3. Batch Adsorption Study and Data Management

Congo Red powder was used to prepare the adsorbate stock solution (1000 mg/L) in this study, while working solutions were subsequently prepared from the stock by serial dilution. Batch adsorption studies were carried out with Congo Red as adsorbate on the G-3PS and G-5PS adsorbents to determine the effects of time, pH, concentration and temperature, as well as adsorbent's reusability. The experimental times range from 10 - 60 min, pH from 5 - 9, concentration from 10 - 22 mg/L and temperature from 25 - 45˚C. Except otherwise stated, the equilibrium time used for the study was 40 min (with the exception of effect of time), 20 mg of G-3PS or G-5PS and 20 mL volume 20 mg/L (except for effect of concentration) of Congo Red solution. The experiments were carried out in replicate.

For a typical batch experiment, the adsorption was done by adding 20 mg of G-3PS or G-5PS into 20 mL Congo Red solution of specified concentration in plastic centrifuge containers.

The G-3PS /G-5PS and 20 mL Congo Red solution mixtures were placed in an orbital shaker at 200 rpm until equilibrium was attained. The solutions pH was adjusted by either 0.1 M HCl or NaOH when necessary. At equilibrium the plastic centrifuge bottles were withdrawn, followed by centrifugation at 4000 rpm for 10 min. The amount of adsorbate (Congo Red) remaining in solution were determined with a Jenway 6,300 spectrophotometer (λ_{max} = 665 nm).

Reusability was carried out using 20 mg of the previously used G-3PS/G-5PS.

The amount of Congo Red adsorbed on G-3PS/G-5PS was desorbed by shaking in 20 mL of desorption solvents (0.1 CH_3COOH, 1 M NaOH and Ultra pure water) at 200 rpm for 40 min and then the desorbed Congo Red analyzed as described above. The G-3PS/G-5PS sample was washed twice with deionized water before being reused. The reuse was carried out twice more.

2.4. Data Management

The amounts of Congo Red adsorbed on G-3PS/G-5PS were calculated using the equation:

$$q_e = \left(C_O - C_e\right)V/m \tag{1}$$

where (C_o) and (C_e) are initial and final concentrations (mg/L), q_e, V and m are the Congo Red amount of adsorbed (mg/g), Congo Red solution volume (mL) and G-3PS/G-5PS mass (g), respectively.

Three kinetics isotherm models [Lagergren [15] Pseudo-First Order (PFO) (Eq. 2), Pseudo-Second Order (PSO) (Eq. 3) [16] [17] kinetics models, and the weber-morris [18] intraparticle diffusion (IPD) (Eq. 4)] were used in describing the effect of time data.

$$q_t = q_e\left(1 - e^{-k_1 t}\right)k_1 \tag{2}$$

$$q_t = \frac{q_e^2 k_2 t}{1 + q_e k_2 t} \tag{3}$$

$$q_e = k_{IPD} t^{1/2} + C \tag{4}$$

The symbols q_e and q_t are the amounts of Congo Red adsorbed (mg/g) on the G-3PS/G-5PS at equilibrium and time t, respectively; and k_1 (/min), k_2 (g/g/min) and k_{IPD} (g/gmin$^{1/2}$) are the rate constants of the PFO, PSO and IPD, respectively; while C (mg/g) is the amount of Congo red adsorbed on the G-3PS/G-5PS surfaces.

Two adsorption isotherm models [the Langmuir [19] (Eq. 5) and Freundlich [20] (Eq. 6)] have been employed to describe the equilibrium data.

$$\frac{C_e}{q_e} = \frac{1}{q_m K_L} + \frac{C_e}{q_m} \tag{5}$$

$$\log q_e = \log K_f + \frac{1}{n}\log C_e \tag{6}$$

Where;

C_e = concentration of adsorbate at equilibrium (mgg^{-1});

K_L = Langmuir constant related to adsorption capacity (mgg^{-1}).

The essential characteristics of the Langmuir isotherm can be expressed by a dimensionless constant called the separation factor R_L [21].

$$S_f = \frac{1}{1 + K_L C_O} \tag{7}$$

Where K_L = Langmuir constant (mgg^{-1});

C_o = Initial concentration of adsorbate (mgg^{-1}).

S_f values indicate the adsorption to be unfavourable when $S_f > 1$.

Linear when $S_f = 1$

Favourable when $0 < S_f < 1$and irreversible when $S_f = 0$

The parameters K_f and n representthe Freundlich model capacity factor and the isotherm linearity parameter, respectively.

Thermodynamic [enthalpy change-ΔH^o (Eq. 7), entropy change-ΔS^o (Eq. 7) and Gibbs free energy-ΔG^o (Eq. 8)] parameters were also estimated.

$$LnK_o = \frac{\Delta S^o}{R} - \frac{\Delta H^o}{RT} \tag{7}$$

$$\Delta G^o = -RTLnK_o \tag{8}$$

The hopping number describes the number of hopping done by the adsorbate molecule while finding a vacant site on the adsorbent surface during sorption processes [22]. The expression relating the hopping number (n) to the surface coverage (θ) is given as:

$$n = \frac{1}{(1-\theta)\theta} \tag{9}$$

3. Results and Discussion

3.1. Physical and Chemical Characterizations

The generic schematic synthesis of the Generation-3/Generation-5 PAMAM functionalized silica (G-3PS/G-5PS) adsorbents is shown in **Figure 1**. In order to prepare these adsorbents, the pristine silica gel (SG) and PAMAM dendrimers were pretreated independently before both were compacted to obtain the final adsorbent. Basically, the APTES was implanted on silica via surface hydroxyl groups resulting in the amino ($-NH_2$) functionalized silica (SG-APTES). After that the G-3/G-5 PAMAM dendrimers were functionalized with succinic anhydride to obtain the carboxylic acid (−COOH) terminated G-3/G-5 PAMAM dendrimers. Finally, the $-NH_2$ group of the SG-APTES and the −COOH group of the succinic acid terminated G-3/G-5 PAMAM dendrimers were combined via an *N*-(3-dimethylaminopropyl)-*N*'-ethylcarbodiimide hydrochloride (EDC) aided coupling reaction ensuing in the G-3/G-5 PAMAM functionalized silica (G-3PS/G-5PS) [23]. Confirmation of the successful synthesis of G-3PS/G-5PS is shown in **Table 1** and **Figure 2**. The pH at point of zero charge (pHpzc) values were observed to be low at 3.1 and 2.9 for G-3PS and G-5PS respectively. Consequently, adsorbent surfaces become predominantly negative above these pH

Table 1. Physicochemical parameters of the synthesized adsorbents.

Adsorbent	pHpzc	BET surface area (m^2/g)	Pore size (cm^2/g)
G-3PS	3.1	16.9	0.073
G-5PS	2.9	4.7	0.026

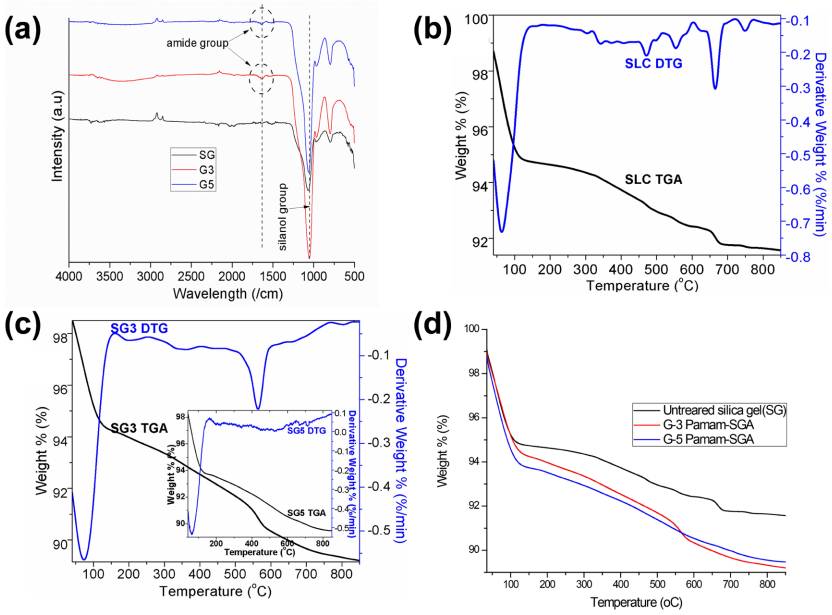

Figure 2. (a) FTIR spectra of SG, G-3PS and G-5PS; TGA and DTA spectra of (b) SG, (c) G-3PS (Insert: G-5PS); (d) comparison of TGA spectra for SG, G-3PS and G-5PS; SEM micrograph of typical G-3PS adsorbent [25].

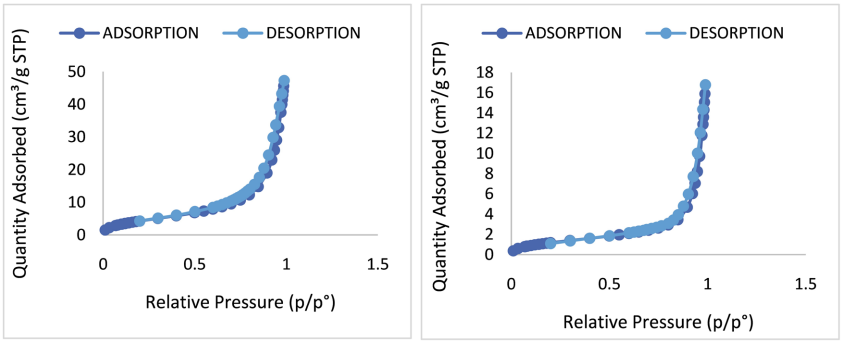

Figure 3. (a) G-3SP-N_2 adsorption-desorption isotherm; (b) G-5SP-N_2 adsorption-desorption isotherm.

values. The N_2-adsorption/desorption isotherm (**Figure 3**) were the classical type IV isotherm, an indication that the G-3PS and G-5PS were mesoporous; the BET surface area were ≤16.9 m^2/g with a relatively large pore width of ≥17.4. The large pore widths may create more space for large contaminant molecules to be sequestrated from solution via pore filling mechanisms [24]. The FTIR spectra of the pure silica (SG), G-3PS and G-5PS adsorbents are shown in **Figure 2(a)**. The typical stretching peaks of the silanol Si-O-Si group were obvious at around 1060 cm^{-1} and 800 cm^{-1} [25], while the evident peak associated with the newly incorporated amide group was observed for the G-3PS and G-5PS at 1630 cm^{-1}.

The TGA spectra are shown in **Figure 2(b)-(d)**. The spectra showed two major thermal transitions for the pure SG, G-3PS and G-5PS adsorbents as temperature was raised from 40 to 900˚C. The first was observed below 150˚C for both

materials (**Figure 2(b)-(c)**) and this was attributed to loss of water molecules that were physically adsorbed within the interlayer of the backbone silica material [24], resulting in about 3.6, 4 and 4% weight losses, respectively. The next thermal transition was observed at 665 °C for SG with a weight loss of 3.5% (**Figure 2(d)**), while it was observed at a lower temperature (≈560˚C) for G-3PS and G-5PS with weight losses of ≈ 4.5% each. The higher weight losses exhibited by G-3PS and G-5PS at lower temperatures were a confirmation of the presence of newly incorporated APTES and PAMAM dendrimer groups which were easily broken down when compared to the backbone silica material. Accordingly, the weight losses at this second thermal transition were attributed to the endothermic decompositions of surface hydroxyl groups on the pure SG, G-3PS and G-5PS as well as the APTES and PAMAM groups.

3.2. Rate and Kinetics of G-3SP and G-5SP Congo Red Adsorption

The outcome of Congo Red adsorption trend on the G-3SP and G-5SP as time varied are shown in **Figure 4**. From this, it was observed that adsorption rates were very fast at the beginning of the experiment to the initial 30 min when the adsorption-desorption rates became stable and equilibria were achieved in both cases. The initial quick adsorption rate was attributed to adsorption on the abundant vacant surface adsorption sites and filling of the pore spaces by Congo Red molecules in solution. After this point, no more significant Congo Red adsorption was possible because accessible adsorption sites have been occupied

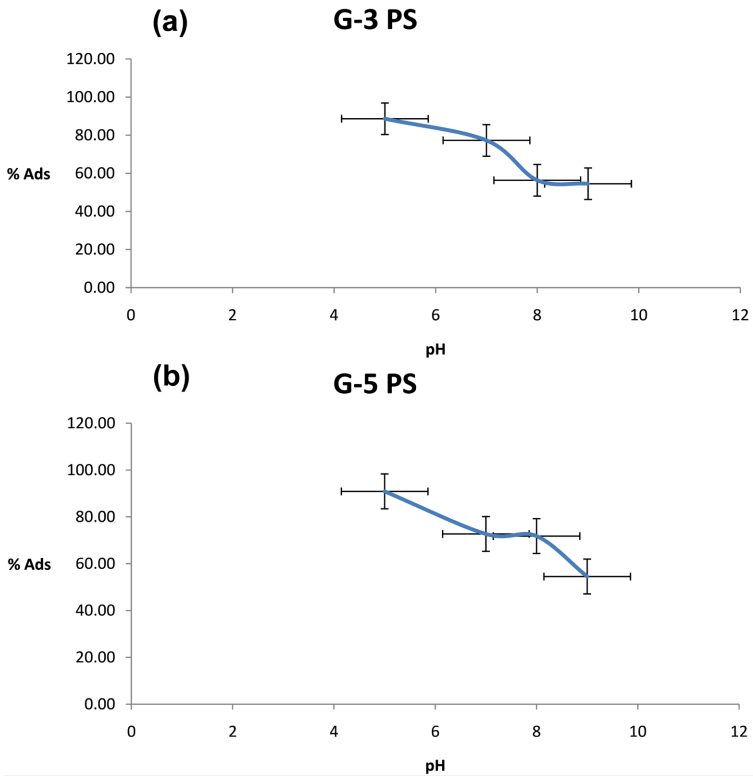

Figure 4. Effect of pH on the uptake of Congo Red.

Table 2. Kinetic model parameters for Congo Red adsorption.

Kinetic model	Parameter	G-3PS	G-5PS
*PFO	q_e (mg/g)	1.05	1.06
	k_1 (/min)	0.39	0.22
	r^2	0.412	0.411
*PSO	q_e (mg/g)	18.726	18.730
	k_2 (g/mg/min)	0.0135	0.0106
	r^2	0.999	0.999
*IPD	C (mg/g)	18.065	18.194
	k_i (g/gmin$^{1/2}$)	0.0843	0.0663
	r^2	0.7327	0.7548
*PPA from IPD	%	3.4	3.1
*PSA from IPD	%	96.6	96.9
Experimental q_e	mg/g	18.78	18.78

[a] Pseudo-first order (PFO) model; *Pseudo-second order (PSO) model; *Intra-particle diffusion (IPD) model; *PPA = Predicted pore adsorption from IPD; PSA = Predicted surface adsorption from IPD.

therefore, equilibrium is believed to have been attained. From these experiments, the time for equilibrium attainment is 30 minutes for G-3PS and 20 minutes G-5PS. Additionally, the time data from these particular experiments were fitted to three adsorption kinetic models; the pseudo-first and second order and the intra-particle kinetic models (results are shown in **Table 2**).

The evaluation of the effect of time on Congo Red adsorption data was carried outby comparing the pseudo-first order and pseudo-second order kinetic models (figures not shown) to the experimental data by using their correlation coefficients (r^2) and the equilibrium adsorption (q_e) values. It was observed that the r^2 value fitting of the pseudo-second order kinetic model was better correlated and predicted the experimental q_e value. Thus, the experimental data fitted the pseudo-second order kinetic model better then the pseudo-first order kinetic model, and may give insight into the adsorption process. This fitting suggests the possible occurrence of chemisorption between Congo Red and the adsorbents (G-3PS/G-5PS). As such the mechanism was mainly electrostatic interactions between the Congo Red molecules and the active functional groups on the G-3PS and G-5PS composites [26] [27]. The intra-particle diffusion kinetic model parameter C (mg/g) provided valuable insights to a better understanding of the surface and pore adsorption of Congo Red dye on the adsorbents. For a C value that is equal to the q_e value, it implied the adsorption was basically a surface phenomenon; but for lower C value, the remaining was attributed to pore adsorption or filling [26]. Consequently, the C value in **Table 2** implied approximately 90% pore filling and 10% surface adsorption. The implication of both surface and pore adsorption of Congo Red on

the adsorbents (G-3SP and G-5SP) from the intra-particle diffusion kinetic model is that the adsorption mechanism may not simply be electrostatic as suggested by the pseudo-second order kinetic model. If this is the case, then the adsorption isotherm model would give further insights on the process.

3.3. Effect of pH on Congo Red Adsorption on G-3PS and G-5PS

The pH of an aqueous solution is a crucial factor in the adsorption of anionic dyes because it has a direct influence on the ionization process of dye molecules as well as the surface binding sites of the adsorbent [27]. Research reports have it that pH affects the charge density surrounding the adsorbent as well as the adsorbate; and this eventually controls the degree of adsorption [28]. Thus, the Congo Red adsorption trend on G-3PS and G-5PS as pH varied from 5 - 9 was examined and results showed in **Figure 4(a)** and **Figure 4(b)** respectively. It was observed that Congo Red removal efficiency decreased from approximately 90.9% to 54.6% with increase in pH of the aqueous solution from pH = 5 through pH = 9. These trends can be explained in terms of the G-3PS and G-5PS pH values at point of zero charge (pHpzc) which were observed to be 3.1 and 2.9. Below the pHpzc, the adsorbent surfaces are blocked by protonation making them uncharged thus, Congo Red removal are mainly possible via pore filling with very small electrostatic attraction; this is the reason for the high adsorption values which corroborates with projection of the intra particle diffusion kinetic model. Congo Red being an acidic dye dissociates to produce negatively charged sulfonic groups ($R\text{-}SO_3^-$) in an acidic medium and the adsorbents being positively charged at the surface at low pH necessitates electrostatic interactions between them (adsorbents) and sulfonic groups ($R\text{-}SO_3^-$). However, with increasing pH, these surface adsorption sites become progressively deprotonated due to the presence of negatively charged hydroxyl groups (OH^-) that compete with sulfonic groups ($R\text{-}SO_3^-$) for available adsorption sites. This leads to marginal uptake of Congo Red molecules (**Figure 4(a)** and **Figure 4(b)**). Similar results have been reported in literature [29] [30] [31] from the experimental result, optimum adsorption was observed at ph = 5 for both G-3PS and G-5PS.

3.4. Adsorption Trends at Varying Time, Adsorbate Concentration and Temperature

Initial Congo Red concentration provides the necessary driving force to surmount the resistance to mass transfer of dye molecules between the bulk adsorbate solution and adsorbent surface [27]. **Figure 5** correlates the percentage uptake of Congo Red by both adsorbents with time, with G-3SP recording 99.03 % adsorption and G-5PS 99.2% adsorption after 30 minutes in both cases. Results of the effect of varying Congo Red concentrations on G-3PS and G-5PS adsorption are depicted as the adsorption trend plots in **Figure 6(a)-(b)**. The trends showed increases in Congo Red adsorption by G-3PS and G-5PS as concentration increased from 10 through 22 mg/L. These trends were also observed for the various temperatures investigated: 25, 35 and 45 ˚C (**Figure 6(a)-(b)**). This trend

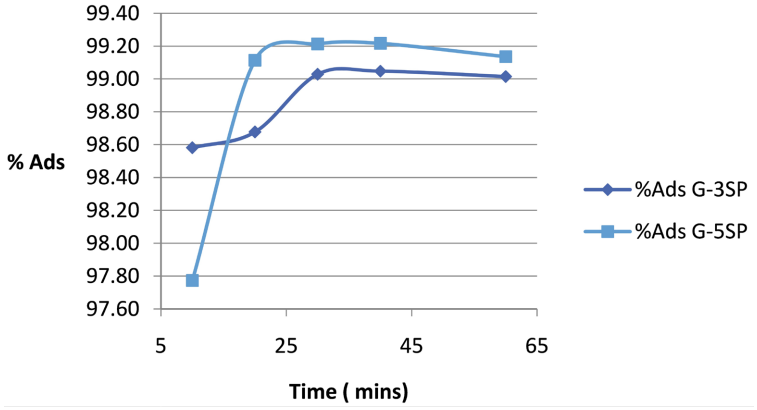

Figure 5. Correlation of adsorbate removal efficiency and time.

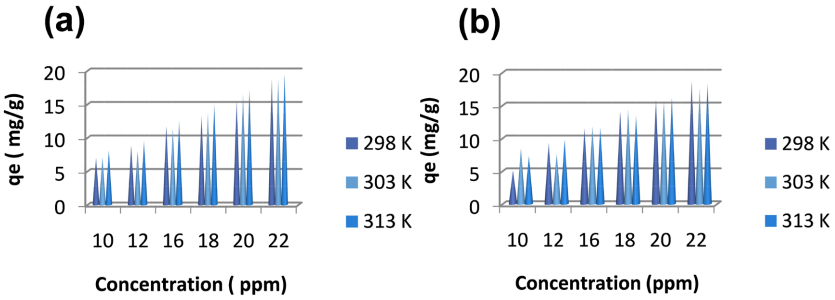

Figure 6. Correlation of adsorbate removal efficiency with various initial concentration (C_O) at different operation temperatures.

may be attributed to the driving force of concentration gradient which affects the behaviour of adsorbate molecules between the external surfaces of the G-3PS and G-5PS and within their internal pores [32] [33]. At equilibrium for a particular aqueous concentration when the movement of adsorbate molecules between adsorbent surfaces (G-3PS/G-5PS) and pores are equal, movement of Congo Red molecules across both boundaries will be notably impermissible. However, increasing the aqueous concentration of the adsorbate re-ignited the migration across both boundaries resulting in the observed higher uptake of adsorbate molecules [34].

Table 3. Adsorption isotherm models parameters for Congo Red.

Adsorption isotherm model	Parameter	G-3PS	G-5PS
Langmuir	q_e (mg/g)	14.86	16.04
	β	20.25	22.58
	r^2	0.998	0.994
	S_f	0.0024	0.0023
Freundlich	n	0.331	0.639
	k_f	5.23	1.07
	r^2	0.999	0.997
Experimental q_e (mg/g)		18.78	18.78

In order to give a better description of the adsorption mechanism involved, the equilibrium Congo Red adsorption data on G-3PS and G-5PS at 45˚C (313 K) were fitted to two adsorption isotherm models: the Langmuir and Freundlich models. Comparison of model parameters in **Table 3** showed that the experimental data fitted the Freundlich adsorption isotherm model better than the Langmuir model. The Freundlich model had a correlation coefficient (r^2) closer to unity (0.999) than the Langmuir (0.998) for G-3PS. Similarly for G-5PS Freundlich showed a slightly higher correlation (0.997) Langmuir (0.994). The Langmuir adsorption isotherm relatively predicted the maximum adsorption capacity (q_e) values for G-3PS and G-5PS as 14.82 mg/g and 16.04 mg/g respectively, these values were close to the experimental q_e values for both adsorbents. The correlation of the experimental data to the Freundlich adsorption isotherm model suggests that the adsorption of Congo Red on G-3PS and G-5PS might have occurred on heterogeneous surfaces and there were multilayer of Congo Red formed on surfaces of unequal energy at equilibrium [17] [35]. This is in contrast to the Langmuir model which assumes that the adsorption of Congo Red occurred on surfaces of equal energy with formation of monolayer of Congo Red on these surfaces at equilibrium.

However, the relatively high r^2 values of the Langmuir isotherm may be explained thus when adsorption occurs in dissimilar sites having approximately equal affinity, they each obey the Langmuir adsorption isotherm model [36]. The combination of these individual Langmuir isotherms results in close approximation to the Freundlich adsorption isotherm model. Also, a critical look at the Freundlich n values in **Table 3** show that these small values which were less than unity (0.331 and 0.639 for G-PS3 and G-5PS, respectively) is a clear indication that the adsorption processes tended towards non-linearity (i.e. more toward the Freundlich than the Langmuir adsorption isotherm). The n values could be considered as an indicator of surface site energy distribution [17]; thus these n values suggest adsorption on heterogeneous adsorption sites with slightly unequal affinity for the adsorbate molecules.

Increasing the ambient experimental temperature from 298 K, 303 K and 313 K (**Figure 7(a)-(b)**) showed that temperature had a helpful effect on the adsorption

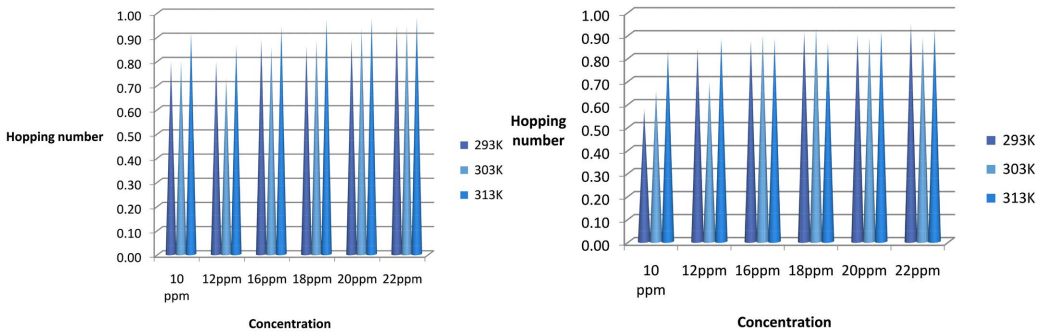

Figure 7. A correlation of hopping number with temperature and concentration (a) Congo Red adsorption on G-3PS; (b) Congo Red adsorption on G-5PS.

Table 4. Thermodynamic parameters of the G-3PS and G-5PS adsorbents for Congo Red adsorption.

Thermodynamic Parameter		G-3PS	G-5PS
ΔH	kJ mol^{-1}	43.07	43.28
ΔS	kJ mol^{-1} K^{-1}	140.42	125.86
ΔG (kJ mol^{-1})	293 K	−39.21	−27.66
	303 K	−40.60	−28.30
	313 K	−41.95	−29.23

of Congo Red molecules on both G-3PS and G-5PS; thus, increasing the temperature, increases Congo Red adsorption. This trend suggests an endothermic process for Congo Red adsorption on the G-3PS and G-5PS adsorbents. In order to ascertain the impact of temperature, adsorption processes were evaluated using thermodynamic parameters (ΔH, ΔS and ΔG) which were calculated from the experimental equilibrum data obtianed at the various temperatures examined and the parameters are shown in **Table 4**. The ΔG values for all temperatures studied were negative, and suggested spontaneous and feasible adsorption processes for Congo Red adsorption on both adsorbents. The value of ΔH obtained from the calculation was positive in both cases and this confirmed the assumption that the adsorption processes were endothermic. For a typical endothermic process, increase in external energy input would favour the forward process (see **Figure 7**); thus, the enhanced Congo Red adsorption with increase in solution temperature. The positive value of the ΔS is an indication of increased randomness of Congo Red molecules in solution as the adsorption processes moved towards equilibrium [25].

3.5. Reusability Study and Comparison with Reported Adsorbents

Desorption studies are very important in two respects; firstly, to understand the possibility of recovering depleted adsorbent and secondly, to elucidate the adsorption mechanism [37] [38]. Accordingly, the reusability of the G-3PS and G-5PS adsorbents were investigated in order to ascertain if their use as adsorbent for Congo Red is cost-effective and also to confirm the proposed adsorption mechanisms. Research reports have it that, if dyes adsorbed on adsorbents are easily desorbed by water, it can be assumed that the links between dye molecules and adsorbent surfaces are weak bonds, if they are desorbed by strong acid or strong base the dye-adsorbent attachment could be due to ion exchange and if organic acid desorbs the dye then it is presumed that the dye-adsorbent link is chemisorption [39]. Accordingly, three cycles of desorption procedures carried out using Acetic acid, Water and Sodium Hydroxide as eluents on previously used G-3PS and G-5PS adsorbents are depicted in **Figure 8(a)-(b)**. This result showed a decreasing trend for Congo Red adsorption in this order.

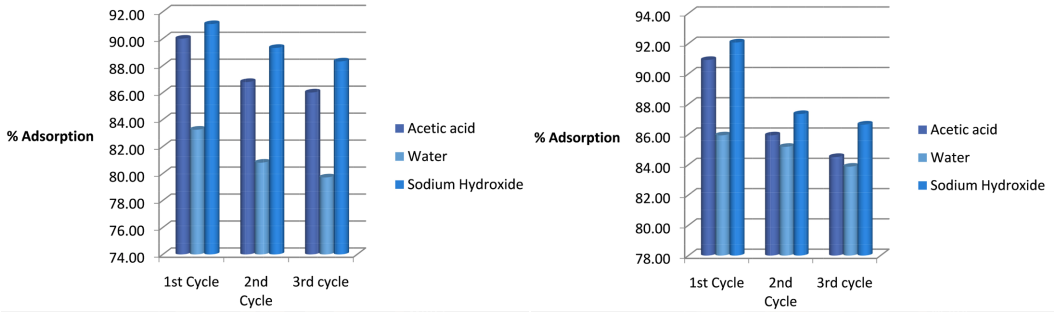

Figure 8. Reusability plots for Congo Red adsorption on (a) G-3PS and (b) G-5PS showing two adsorption cycles for three desorbing solvents.

G-3PS

1st cycle: NaOH (91%) > Acetic acid (90%) > Distilled water (83%)

2nd cycle: NaOH (89%) > Acetic acid (86%) > Distilled water (80%)

3rd cycle: NaOH (88%) > Acetic acid (79%) > Distilled water (79%)

G-5PS

1st cycle: NaOH (92%) > Acetic acid (90%) > Distilled water (85%)

2nd cycle: NaOH (87%) > Acetic acid (86%) > Distilled water (85%)

3rd cycle: NaOH (86%) > Acetic acid (84%) > Distilled water (83%)

This shows NaOH is a more efficient eluents compared to Acetic acid and distilled water. However, all three eluents achieved high desorption efficiency. Thus, it is evident that dye-adsorbent links could be predominantly via ion exchange because partial desorption of dyes with a change in pH is indicative of electrostatic interactions [40]. As such chemisorption seems to be one of the primary mechanisms of adsorption since incomplete desorption of the dye has been observed [41]. The roles of Acetic acid and distilled water as eluents in the desorption experiments suggests electrostatic linkages (chemisorption) and hydrogen bonds (physisorption) as part of the dye-adsorbent linkages [37].

The higher adsorption recorded for the first adsorption processes were attributed to the empty adsorption sites available on G-3PS and G-5PS. After the first adsorption process, desorption of the surface adsorbed Congo Red molecules were simple because the desorbing reagents could easily access the surface. However, the Congo Red molecules within the pores or crevices of both adsorbents were difficult to access and thus desorption of the adsorbates molecules from these parts and was unfeasible. This implies that in the subsequent adsorption cycles, the pores or crevices became inaccessible leading the lowered and nearly constant adsorption capacity recorded.

The G-3PS and G-5PS adsorption capacity for Congo Red have been compared with some other adsorbents reported in the literature (**Table 5**). The comparison showed that both adsorbents performed well when compared with other reported adsorbents previously used for Congo Red adsorption. The fact that the adsorption capacity values of both adsorbents were comparable to some of the best performing adsorbents reported in literature reveals the potential of these adsorbents for removal of Congo Red from real wastewater.

Table 5. Comparison of G-3PS and G-5PS Congo Red adsorption capacity with some adsorbents reported in literature.

Adsorbent	qe (mg/g)	Reference
G-3PS	14.86	This study
G-5PS	16.04	This study
AC from Coir Pith	6.72	[42]
Datestone AC (CO2800)	15.23	[43]
Activated Carbon Coffee waste	90.90	[27]
Luffa cylindrica cellulose fibre	17.39	[44]
Anilinepropylsilica xerogel	22.62	[45]
Eucalyptus Wood Sawdust	31.25	[46]
Eichhhonia Charcoal	56.8	[47]
Bottom Ash	142.1	[48]
Magenetite FeO_4 Core shell NPs	11.22	[49]
Bimetallic Fe-Zn NPs	28.56	[50]
Glutaraldehyde cross-linked magnetite chitosan	101.74	[51]
Microgel based on nano-cellulose polyvinyl amine	869.1	[52]
Malachite-Clay nanocomposite	238.09	[53]
Polyaniline-montmorrillonite composite	25.1	[54]
Magemite nanoparticles	208.33	[55]
Zinc oxide nanorods loaded on activated carbon	142.9	[56]
Cu-NPs	37.5	[57]
Amino-coated Fe_3O_4 nanoparticles	97.3	[58]

4. Conclusions

Generation-3 and 5 polyamidoamine (PAMAM) dendrimers were implanted on Silica using of a (3-aminopropyl) triethoxysilane (APTES) linkage to obtain a G3/G5-PAMAM functionalized silica (G-3PS/G-5PS). Both adsorbents (G-3PS/G-5PS) were characterized and explored for Congo Red removal from aqueous solution. The characterization results showed the accomplishment of the synthesis owing to the occurrence of FTIR peak associated with amide group, larger pore sizes in comparison to unmodified silica with slightly lower thermal stability due to the presence of the integrated groups.

Further G-3PS and G-5PS showed a fast equilibrium time of 30 and 20 minutes respectively for Congo Red adsorption, optimum adsorption pH of 5 and experimental Congo Red adsorption capacity values of 14.86 and 16.04 mg/g, respectively; performances measured up with adsorbent materials reported in the literature. Experimental data and calculated thermodynamic variables indicated spontaneous, feasible and endothermic adsorption processes in both cases. The adsorption isotherm modeling parameters suggested Congo Red removal mechanism involving dissimilar adsorption happening majorly on adsorbents

surfaces (≈96.75%) and within the pores (≈3.25%). The G-3PS and G-5PS exhibited very good reusability even after the three adsorption cycles maintaining more than 80% of their adsorption capacity values for all three desorption solvents used. NaOH proved to be the most efficient desorption solvent out of the three solvents used (CH_3COOH, H_2O and NaOH). Based on the results obtained it is evident that the Congo Red-Adsorbent link could be predominantly via ion exchange and physisorption because NaOH (a strong base) gave the best result. The impact of acetic acid as a desorption solvent points at the role of chemisorption in the uptake of Congo Red by GG-3PS and G-5SP. Water also gave a good account on its ability to desorb Congo Red from both adsorbents thus, it is presumed that some weak bonds (hydrogen bonds) c could be part of the Congo Red-adsorbent linkages [37] [41]. These facts bring to bear the potentials of both adsorbents for removal of Congo Red from real wastewater.

Conflicts of Interest

The authors declare no conflicts of interest regarding the publication of this paper.

References

[1] Pearce, C.L., Lloyd, J.R. and Guthrie, J.T. (2003) The Removal of Colour from Textile Waste Water Using Whole Bacterial Cells: A Review. *Dyes and Pigments*, **58**, 179-196. https://doi.org/10.1016/S0143-7208(03)00064-0

[2] McMullan, G., Meehan, C., Conneely, A., Nirby, N., Robinson, P., Nigam, I., Bannat, M. and Marchant, S.W.F. (2001) Minireview: Microbial Decolorization and Degradation of Textile Dyes. *Applied Microbiology and Biotechnology*, **56**, 81-87. https://doi.org/10.1007/s002530000587

[3] Munagapati, S. and Kim, D.S. (2016) Adsorption of Anionic Azo Dye Congo Red from Aqueous Solution by Cationic Modified Orange Peel Powder. *Journal of Molecular Liquids*, **20**, 540-548. https://doi.org/10.1016/j.molliq.2016.04.119

[4] Finar, I.L. (1986) Organic Chemistry Vol. 1. 5th Edition, Longman Group Ltd, London, 884-885.

[5] Bahl, A. and Bahl, B.S. (2010) Advanced Organic Chemistry S. Chand & Company Ltd, New Adhi.

[6] Han, R.P., Han, P., Cai., Z.H. Zhao, Z.H. and Tang, M.S. (2008) Kinetics and Isotherms of Neutral Red Adsorption on Peanut Husk. *Journal of Environmental Science*, **20**, 1035-1041. https://doi.org/10.1016/S1001-0742(08)62146-4

[7] Siddiqui, S.I., Allehyani, E.S., Al-Harbi, S.A., Hasan, Z., Abomuti, M.A., Rajor, H.K. and Oh, S. (2023) Investigation of Congo Red Toxicity towards Different Living Organisms: A Review. *Processes*, **11**, Article 807. https://doi.org/10.3390/pr11030807

[8] Katheresan, V., Kansedo, J., and Sie Yon, J.L. (2018) Efficiency of Various Recent Wastewater Dye Removal Methods: A Review. *Journal of Environmental Chemical Engineering*, **6**, 4676-4697. https://doi.org/10.1016/j.jece.2018.06.060

[9] Kanday, A., Marrachi, F., Asif, M. and Hameed, B.H. (2017) Mesoporous Zeolite-Activated Carbon Composite from Oil Palm Ash as an Effective Adsorbent for Methylene Blue. *Journal of Taiwan Institute of Chemical Engineering*, **70**, 32-41.

https://doi.org/10.1016/j.jtice.2016.10.029

[10] Diagboya, P.N. and Dikio, E.D. (2018) Silica-Based Mesoporous Materials; Emerging Designer Adsorbents for Aqueous Pollutants Removal and Water Treatment. *Microporous and Mesoporous Materials*, **266**, 252-267. https://doi.org/10.1016/j.micromeso.2018.03.008

[11] Miguez, J.P., Gama, R.S., Bolina, I.C.A., De Melo, C.C., Cordeiro, M.R., Hirata, D.B. and Mandes, A.N. (2018) Enzymatic Synthesis Optimization of a Cosmetic Ester Catalyzed by a Home Made Biocatalyst Prepared *via* Physical Adsorption Lipase on Amino-Functionalized Rice Husk Silica. *Chemical Engineering Research and Design*, **139**, 296-308. https://doi.org/10.1016/j.cherd.2018.09.037

[12] Acres, R.G., Ellis, A.V., Alvino, J., Lenahan, C.E., Khodakov, D.A., Metha, G.F. and Andersson, G.G. (2012) Molecular Structure of 3-Aminopropyltriethoysilane Layers Formed on Silanol-Terminated Silicon Surfaces. *The Journal of Physical Chemistry A*, **116**, 6289-6297. https://doi.org/10.1021/jp212056s

[13] Shi, X., Sun, K., Balogh, P.L. and Baker Jr., R.J. (2006) Synthesis, Characterization, and Manipulation of Dendrimer-Stabilized Iron Sulfide Nanoparticles. *Nanotechnology*, **17**, 4554. https://doi.org/10.1088/0957-4484/17/18/005

[14] Jiang, Y., Gao, Q., Yu, H., Chen, Y. and Deng, F. (2007) Intensively Competitive Adsorption for Heavy Metal Ions by PAMAM-SBA-15 and EDTA-PAMAM-SBA-15 Inorganic-Organic Hybrid Materials. *Microporous and Mesoporous Materials*, **103**, 316-324. https://doi.org/10.1016/j.micromeso.2007.02.024

[15] Lagergren, S.K. (1898) About the Theory of So-Called Adsorption of Soluble Substances. *Handlinge*, **24**, 147-156.

[16] Haerifar, M. and Azizian, S. (2014) Fractal-Like Kinetics for Adsorption on Heterogeneous Solid Surfaces. *The Journal of Physical Chemistry C*, **118**, 1129-1134. https://doi.org/10.1021/jp4110882

[17] Ayawei, N., Ebelegi, N.A. and Wankasi, D. (2017) Modeling and Interpretation of Adsorption Isotherms. *Journal of Chemistry*, **2017**, Article ID: 3039817. https://doi.org/10.1155/2017/3039817

[18] Weber, W.J. Morris, J.C. and Sanit, J. (1963) Kinetics of Adsorption on Carbon from Solution. *Journal of the Sanitary Engineering Division*, **89**, 31-60. https://doi.org/10.1061/JSEDAI.0000430

[19] Langmuir, I. (1916) The Constitution and Fundamental Properties of Solids and Liquids. Part I. Solids. *Journal of the American Chemical Society*, **38**, 2221-2295. https://doi.org/10.1021/ja02268a002

[20] Freundlich, H.M.F. (1906) Over the Adsorption in Solution. *The Journal of Physical Chemistry*, **57**, 1100-1107.

[21] Ayawei, N., Angaye, S.S., Wankasi, D. and Dikio, E.D. (2015) Synthesis, Characterization and Application of Mg/Al Layered Double Hydroxide for the Degradation of Congo Red in Aqueous Solution. *Open Journal of Physical Chemistry*, **5**, 56-70. https://doi.org/10.4236/ojpc.2015.53007

[22] Horsfall, M. and Spiff, I.A. (2005) Effect of 2–Mercaptoethanoic Acid Treatment of Fluted Pumpkin Waste (*Telfairia occidentalis* Hook. F.) on the Sorption of Ni^{2+} Ions from Aqueous Solutions. *Journal of Scientific & Industrial Research*, **64**, 613-620.

[23] Diagboya, P.N., Olu-Owolabi, B.I., Zhou, D. and Han, B.H. (2014) Graphene Oxide—Tripolyphosphate Hybrid Used as a Potent Sorbent for Cationic Dyes. *Carbon*, **79**, 174-182. https://doi.org/10.1016/j.carbon.2014.07.057

[24] Diagboya, P.N., Olu-Owolabi, B.I. and Adebowale, K.O. (2014) Microscale Scavenging of Pentachlorophenol in Water Using Amine and Tripolyphosphate-Grafted

SBA-15 Silica: Batch and Modeling Studies. *Journal of Environmental Management*, **146**, 42-49. https://doi.org/10.1016/j.jenvman.2014.04.038

[25] Ebelegi, A.N., Ayawei, N., Inengite, A.K. and Wankasi, D. (2020) Generation-3 Polyamidoamine Dendrimer-Silica Composite: Preparation and Cd (II) Removal Capacity. *Journal of Chemistry*, **2020**, Article ID: 6662402. https://doi.org/10.1155/2020/6662402

[26] Abasi, C.Y., Diagboya, P.N. and Dikio, E.D. (2019) Layered Double Hydroxide of Cobalt-Zinc-Aluminium Intercalated with Carbonate Ion: Preparation and Pb (II) Ion Removal Capacity. *International Journal of Environmental Studies*, **76**, 251-265. https://doi.org/10.1080/00207233.2018.1517935

[27] Lafi, R., Montasser, I. and Hafiane, A. (2018) Adsorption of Congo Red De from Aqueous Solutions B Prepared Activated Carbon with Oxgen-Containing Functional Groups and Its Regression. *Adsorption Science and Technology*, **37**, 160-181. https://doi.org/10.1177/0263617418819227

[28] Xia, C., Jing, Y., Jia, Y., Yue, D., Ma, J. and Xiaojie, Y. (2011) Adsorptionproperties of Congo Red from Aqueous Solution on Modified Hectorite: Kinetic and Thermodynamic Studies. *Desalination*, **265**, 81-87. https://doi.org/10.1016/j.desal.2010.07.035

[29] Purkait, M.K., Maiti, A. and Dasgupta, S. (2007) Removal of Congo Red Using Activated Carbon and Its Regeneration. *Journal of Hazardous Materials*, **1445**, 287-295. https://doi.org/10.1016/j.jhazmat.2006.11.021

[30] Luis, S., Ding, Y. and Li, P. (2014) Adsorptionof Anionic Congo Red from Aqueous Solution Ontonatural Zeolite Modified with N, N-Dimethyl Dehydroabietylamine Oxide. *Chemical Engineering Journal*, **248**, 135-144. https://doi.org/10.1016/j.cej.2014.03.026

[31] Diagboya, P.N. and Dikio, E.D. (2018) Scavenging of Aqueous Toxic Organic and Inorganic Cations Using Novel Facile Magneto-Carbon Black-Clay Composite Adsorbent. *Journal of Cleaner Production*, **180**, 71-80. https://doi.org/10.1016/j.jclepro.2018.01.166

[32] Mohammadi, N., Khani, H., Gupta, V.K., *et al.* (2011) Adsorption Process of Methyl Orange Dye onto Mesoporous Carbon Material—Kinetic and Thermodynamic Studies. *Journal of Colloid and Interface Science*, **362**, 457-462. https://doi.org/10.1016/j.jcis.2011.06.067

[33] Namasivayam, C. and Kavitha, D. (2002) Removal of Congo Red from Water by Adsorption onto Activated Carbon Prepared from Coir Pith, An Agricultural Solid Waste. *Dyes and Pigments*, **54**, 47-58. https://doi.org/10.1016/S0143-7208(02)00025-6

[34] Chukwuemeka-Okorie, H.O., Ekemezie, P.N., Akpomie, K.G. and Olikagu, C.S. (2018) Calcined Corncob-Kaolinite Combo as New Sorbent for Sequestration of Toxic Metal Ions from Polluted Aqua Media and Desorption. *Frontiers in Chemistry*, **6**, Article 273. https://doi.org/10.3389/fchem.2018.00273

[35] Ebelegi, N.A., Angaye, S.S., Ayawei, N. and Wankasi, D. (2017) Removal of Congo Red from Aqueous Solutions Using Fly Ash Modified with Hydrochloric Acid. *Current Journal of Applied Science and Technology*, **20**, 1-7. https://doi.org/10.9734/BJAST/2017/29880

[36] Olu-Owolabi, B.I., Diagboya, P.N. and Adebowale, K.O. (2014) Evaluation of Pyrene Sorption-Desorption on Tropical Soils. *Journal of Environmental Management*, **137**, 1-9. https://doi.org/10.1016/j.jenvman.2014.01.048

[37] Rani, K.C., Naik, A., Chaurasiya, R.S. and Raghavarao, K.S.M.S. (2017) Removal of

Toxic Congo Red Dye from Water Employing Low-Cost Coconut Residual Fiber. *Water Science & Technology*, **75**, 2225-2236. https://doi.org/10.2166/wst.2017.109

[38] Dawood, S. and Sen, T.K. (2012) Removal of Anionic Dye Congo Red from Aqueous Solution by Raw Pine and Acid-Treated Pine Cone Powder as Adsorbent: Equilibrium, Thermodynamic, Kinetics, Mechanism and Process Design. *Water Research*, **46**, 1933-1946. https://doi.org/10.1016/j.watres.2012.01.009

[39] Mall, I.D., Srivastava, V.C., Agarwai, N.K. and Mishra, I.M. (2005) Removal of Congo Re from Aqueous Solution by Bagasse Fly Ash and Activated Carbon: Kinetic Study and Equilibrium Isotherm Analysis. *Chemosphere*, **4**, 492-501. https://doi.org/10.1016/j.chemosphere.2005.03.065

[40] Reddy, M.S., Sivaramakrishna, L. and Reddy, A.V. (2012) The Use of An Agricultural Waste Material, Jujuba Seeds for the Removal of Anionic Dye (Congo Red) from Aqueous Medium. *Journal of Hazardous Materials*, **203**, 118-127. https://doi.org/10.1016/j.jhazmat.2011.11.083

[41] Barragán, B.E., Costa, C. and Marquez, M.C. (2007) Biodegradation of Azo Dyes by Bacteria Inoculated on Solid Media. *Dyes and Pigments*, **75**, 73-81. https://doi.org/10.1016/j.dyepig.2006.05.014

[42] Namasivayam, C. and Arasi, D.J.S.E. (1997) Removal of Congo Red from Wastewater by Adsorption onto Waste Red Mud. *Chemosphere*, **34**, 401-417. https://doi.org/10.1016/S0045-6535(96)00385-2

[43] Bouchemal, N., Merzougui, Z. and Addoun, F. (2011) Adsorption in Aqueous Media of Two Dyes on Activated Carbons Based on Date Stones. *Journal of the Algerian Society of Chemistry*, **21**, 1-14.

[44] Gupta, V.K., Pathania, D., Agarwal, S. and Sharma, S. (2014) Amputation of Congo Red Dye from Waste Water Using Microwave Induced Grafted *Luffa cylindrica* Cellulosic Fiber. *Carbohydrate Polymers*, **111**, 556-566. https://doi.org/10.1016/j.carbpol.2014.04.032

[45] Praven, F.A., Dias, S.L.R., Lim, E.C. and Benvenutti, E.V. (2008) Removal of Congo Red from Aqueous Solution Using by Anilinepropylsilia Xerogel. *Dyes and Pigments*, **76**, 64-69. https://doi.org/10.1016/j.dyepig.2006.08.027

[46] Mane, V.S. and Babu, P.V.V. (2013) Kinetic and Equilibrium Studies on the Removal of Congo Red from Aqueous Solution Using Eucalyptus Wood (*Eucalyptus globulus*) Saw Dust. *Journal of the Taiwan Institute of Chemical Engineers*, **44**, 81-88. https://doi.org/10.1016/j.jtice.2012.09.013

[47] Kaur, S., Rani, S. and Mahajan, R.K. (2013) Adsorption Kinetics for the Removal of Hazardous Dye Congo Red by Biowaste Materials as Adsorbents. *Journal of Chemistry*, **2013**, Article ID: 628582. https://doi.org/10.1155/2013/628582

[48] Mittal, A., Mittal, J., Malviya, A. and Gupta, V.K. (2009) Adsorptive Removal of Hazardous Anionic Dye "Congo Red" from Wastewater Using Waste Materials and Recovery by Desorption. *Journal of Colloid and Interface Science*, **340**, 16-26. https://doi.org/10.1016/j.jcis.2009.08.019

[49] Zhang, Z. and Kong, J. (2011) Novel Magnetic Fe3O4@C Nanoparticles as Adsorbents for Removal of Organic Dyes from Aqueous Solution. *Journal of Hazardous Materials*, **193**, 325-329. https://doi.org/10.1016/j.jhazmat.2011.07.033

[50] Gautam, R.K., Rawat, V., Banerjee, S., Sanroman, M.A., Soni, S., Singh, S.K. and Chattopadhyaya, M.C. (2015) Synthesis of Bimetallic Fe-Zn Nanoparticles and Its Application towards Adsorptive Removal of Carcinogenic Dye Malachite Green and Congo Red in Water. *Journal of Molecular Liquids*, **212**, 227-236. https://doi.org/10.1016/j.molliq.2015.09.006

[51] Zhou, Z., Lin, S., Yue, T. and Lee, T.C. (2014) Adsorption of Food Dyes from Aqueous Solution by Glutaraldehyde Cross-Linked Magnetic Chitosan Nanoparticles. *Journal of Food Engineering*, **126**, 133-141. https://doi.org/10.1016/j.jfoodeng.2013.11.014

[52] Jin, L., Sun, Q., Xu, Q. and Xu, Y. (2015) Adsorptive Removal of Anionic Dyes from Aqueous Solutions Using Microgel Based on Nanocellulose and Polyvinylamine. *Bioresource Technology*, **197**, 348-355. https://doi.org/10.1016/j.biortech.2015.08.093

[53] Srivastava, V. and Sillanpaa, M. (2017) Synthesis of Malachite@Clay Nanocomposite for Rapid Scavenging of Cationic and Anionic Dyes from Synthetic Wastewater. *Journal of Environmental Sciences*, **51**, 97-110. https://doi.org/10.1016/j.jes.2016.08.011

[54] Karthikaikumar, S., Karthikeyan, M. and Kumar, K.K.S. (2014) Removal of Congo Red Dye from Aqueous Solution by Polyaniline-Montmorrillonite Composite. *Chemical Science Review and Letters*, **2**, 606-614.

[55] Afkhami, A. and Moosavi, R. (2010) Adsorptive Removal of Congo Red, A Carcinogenic Textile Dye, from Aqueous Solutions by Maghemite Nanoparticles. *Journal of Hazardous Materials*, **174**, 398-403. https://doi.org/10.1016/j.jhazmat.2009.09.066

[56] Ghaedi, M., Biyareh, M.N., Kokhdan, S.N., Shamsaldini, S., Sahraei, R., Daneshfar, A. and Shahriyar, S. (2012) Comparison of the Efficiency of Palladium and Silver Nanoparticles Loaded on Activated Carbon and Zinc Oxide Nanorods Loaded on Activated Carbon as New Adsorbents for Removal of Congo Red from Aqueous Solution: Kinetic and Isotherm Study. *Materials Science and Engineering*: *C*, **32**, 725-734. https://doi.org/10.1016/j.msec.2012.01.015

[57] Rouhollah, K., Batoul, R., Ghodsieh, B. and Maryam, M. (2018) Green Synthesis of Copper Nanoparticles by Fruit Extract of *Ziziphus spina-christi* (L.) Willd.: Application for Adsorption of Triphenylmethane Dye and Antibacterial Assay. *Journal of Molecular Liquids*, **255**, 541-549. https://doi.org/10.1016/j.molliq.2018.02.010

[58] Dai, R., Zhang, Y., Shi, Z.Q., Yang, F. and Zhao, C.S. (2018) A Facile Approach towards Amino-Coated Ferroferric Oxide Nanoparticles for Environmental Pollutant Removal. *Journal of Colloid and Interface Science*, **513**, 647-657. https://doi.org/10.1016/j.jcis.2017.11.070